25/10/2022]. See the Terms and Conditions (https://colimiestry-europe.onlinelibrary.wiley.com/doi/10.1002/chem.202104102 by Texas Tech University Libraries, Wiley Online Library or [25/10/2022]. See the Terms and Conditions (https://onlinelibrary.wiley.com/mems-and-conditions) on Wiley Online Library for rules of use; OA articles are governed by the applicable Creative Commons is

www.chemeurj.org



# Asymmetric Catalytic Assembly of Triple-Columned and Multilayered Chiral Folding Polymers Showing **Aggregation-Induced Emission (AIE)**

Jia-Yin Wang<sup>+,[a]</sup> Yao Tang<sup>+,[b]</sup> Guan-Zhao Wu<sup>+,[a,b]</sup> Sai Zhang,<sup>[b]</sup> Hossein Rouh,<sup>[b]</sup> Shengzhou Jin, [a] Ting Xu, [a] Yu Wang, [a] Daniel Unruh, [b] Kazimierz Surowiec, [b] Yanzhang Ma, [c] Yunze Li, [d] Courtney Katz, [e] Hongjun Liang, [e] Weilong Cong, [d] and Guigen Li\*[a, b]

Abstract: Unprecedented chiral multilayer folding 3D polymers have been assembled and regulated by uniform and differentiated aromatic chromophore units between naphthyl piers. Screening catalysts, catalytic systems and monomers were proven to be crucial for asymmetric catalytic Suzuki-Miyaura polycouplings for this assembly. X-ray crystallography of the corresponding dimers and trimers revealed the absolute configuration and the intermolecular packing pattern. Up to 61 960  $M_{\rm w}/41$  900  $M_{\rm n}$  and m/z 4317 for polymers and oligomers, as confirmed by gel permeation chromatography (GPC) and MALDI-TOF MS, indicated that these frameworks were composed of multiple stacked layers. The resulting multiple  $\pi$ -assemblies exhibited remarkable optical properties in aggregated states (photoluminescence in solids and aggregation-induced emission in solutions), as well as reversible redox properties in electrochemical performance.

#### Introduction

Multilayer chirality has existed in nature from the beginning of life on Earth. It plays crucial roles in controlling the functions of biomolecules, such as nucleic acids (DNA/RNA) and proteins in human beings, animals, and plants. [1,2] Tremendous progress on chirality in scientific and public communities has been witnessed since Watson and Crick elucidated the DNA doublehelix structure in the 1950s.[1] Meanwhile, inter- and intra-

[a] J.-Y. Wang, G.-Z. Wu, S. Jin, T. Xu, Y. Wang, Prof. Dr. G. Li Institute of Chemistry and BioMedical Sciences School of Chemistry and Chemical Engineering Nanjing University, Nanjing, 210093 (P. R. China) E-mail: Guigen.li@ttu.edu

- [b] Y. Tang, G.-Z. Wu, S. Zhang, H. Rouh, D. Unruh, K. Surowiec, Prof. Dr. G. Li Department of Chemistry and Biochemistry Texas Tech University Lubbock, TX 79409-1061 (USA)
- [c] Prof. Dr. Y. Ma Mechanical Engineering, Texas Tech University Lubbock, TX 79409 (USA)
- [d] Y. Li, Prof. Dr. W. Cong Department of Industrial Engineering Texas Tech University Lubbock, TX 79409-3061 (USA)
- [e] C. Katz, Prof. Dr. H. Liana Department of Cell Physiology and Molecular Biophysics School of Medicine Texas Tech University Health Sciences Center Lubbock, TX 79430-6551 (USA)
- [+] These authors contributed equally to this work.
- Supporting information for this article is available on the WWW under https://doi.org/10.1002/chem.202104102

molecular multilayer  $\pi$ - $\pi$  interactions have attracted extensive interest in biomedical and material sciences.[3,4] For example, the energetics of the H<sup>+</sup>/2e<sup>-</sup> transferring was proven to occur between planar nicotinamide adenine dinucleotide (NADH) and protein-bound flavin (FMN) cofactors, which was responsible for further triggering reduction of nearby FeS centers of pump proteins. [5] Femtosecond mid-infrared spectroscopy indicated that covalently held and slip-stacked terrylene-3,4:11,12bis(dicarboximide) (TDI) led to interesting electronic states of a singlet exciton and two triplet excitons. [6] In modern materials research, helical chirality has been actively explored with a great progress made on novel photo-optical properties for chiral switches, circularly polarized light generation, liquid crystallization, asymmetric catalysis, etc.<sup>[7,8]</sup> Surprisingly, the work on multiple-decked and tightly compacted chiral polymers has been remained uncharted. [9,10] This is probably due to the fact that it is extremely difficult to render asymmetric polymerization and catalytic conditions for the assemblies.[11-14]

Very recently, our laboratories have reported a new form of multilayer 3D chirality which was stacked and spaced primarily by aromatic-aromatic interactions.<sup>[15]</sup> This chirality is different from the traditional planar or helical skeletons and displays unique characteristics of rotational stereoisomerism. Our first multilayer chirality was originated from the group-assistedpurification (GAP) chemistry, relying on C-N bonding anchors through dual Buchwald-Hartwig cross-coupling, and took on new pseudo- $C_2$  symmetry (a, Figure 1A). [16-18] We then developed this new finding to more prevalent C-C bonding bridges (b and c, Figure 1A) with stereochemistry controlled by chiral auxiliaries and catalysts.

The resulting chiral multilayer 3D compounds displayed intriguing macrochirality phenomenon and strong lumines-

5213765, 20

2, 7, Dwarloaded from thts://schemisty-erope.onlinelibrary.wiely.com/doi/10.1002/chem.202104102 by Texas Tech University Libraries, Wiley Online Library on [25/10.2022]. See the Terms and Conditions (https://onlinelibrary.wiley.com/terms-and-conditions) on Wiley Online Library or rules of use; OA articles are governed by the applicable Creative Commons Licensea

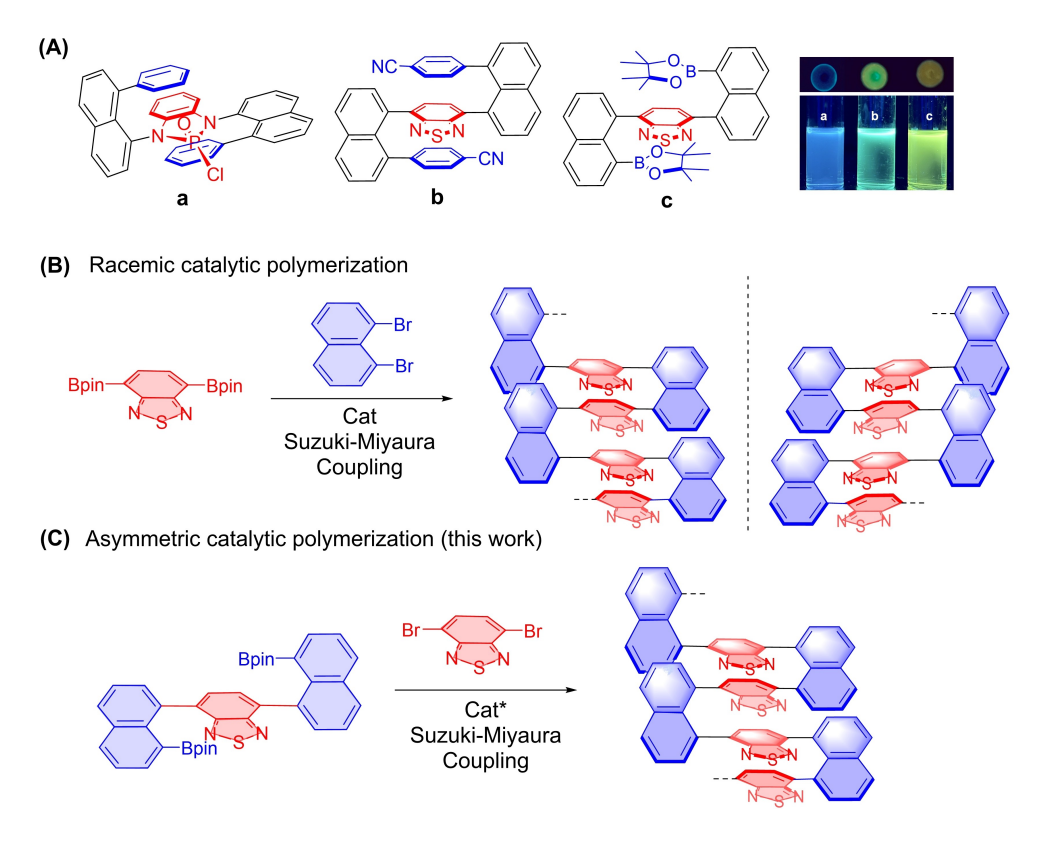


Figure 1. A) Multilayer small molecules; inset: the emission under 365 nm UV irradiation (top: aggregated state on TLC plates; bottom: dilute solutions in CH<sub>2</sub>Cl<sub>2</sub>). B) Formation of racemic polymers. C) Asymmetric catalytic polymerization. Cat\*: chiral catalysts.

cence under UV irradiation in both aggregated state and diluted solutions (Figure 1A, inset).

Based on the above work, we investigated polymerizations leading to structurally compacted triple-columned/multilayered polymers and oligomers along with the corresponding aggregation-induced emission (AIE) properties and computational studies. Multistep Suzuki-Miyaura cross-coupling[19] has been proven to be efficient in one-pot strategy for this polymerization (Figure 1B).[15a] Interestingly, regular loops on the surfaces of vials were observed when the solution of certain trimer was slowly evaporated in the open air, which provided a macro clue of the ordered intermolecular stacking.[20] In this work, we would like to disclose our preliminary results on asymmetric catalytic polymerization providing access to chiral triple-columned/multiple-layered polymers (Figure 1C).

#### **Results and Discussion**

Unlike the racemic design which was involved in uniformed aromatic bridges (red segment, Figure 1B), this work resulted in chiral multilayer folding 3D polymers with altered aromatic bridges between two naphthyl wings. Based on the retrosynthetic analysis (RSA),[21] the representative target 1 C can be disassembled into three synthon pairs as shown in Figure 2A. The cooperations of the first two synthon co-monomers (Figure 2A-I and II) did not yield any stereoselectivity as discussed below, whereas the adjustments of coupling sites shown in Figure 2A-III made adequate improvement on both stereoselectivity and yield.

The synthesis of monomer 1 was started from 4,7bis(4,4,5,5-tetramethyl-1,3,2-dioxaborolan-2-

yl)benzo[c][1,2,5]thiadiazole under classic Suzuki-Miyaura crossconditions followed by reacting bis(pinacolato)diboron. [15b] Selenodiazoles derivatives 2 and 6 served as two additional monomers obtained by following a literature procedure (Figure 2B). [22,23] The reasons for choosing thiadiazole and selenodiazole infrastructures are based on the fact that they are among the most useful scaffolds in polymer and material science. [24,25]

Our first attempt at synthesizing chiral polymers was to perform the reaction of 1,8-dibromonaphthalene with 2,2'-(2,5dimethoxy-1,4-phenylene)bis(4,4,5,5-tetramethyl-1,3,2-dioxaborolane) by applying a series of chiral catalysts including both mono- and bidentate chiral phosphine ligands and Pd-ligand complexes.[15e] Unfortunately, none of these chiral choices catalyzed the present polymerization, giving either no polymeric products or apparent optical rotations for the complex mixtures. We then turned over to screen more suitable monomers. Although the polymerization between the synthons in Figure 2A-II failed to deliver effectiveness, switching the positions of -Br and -Bpin was found to be processed successfully under the same conditions (Figure 2A-III). Among the examined chiral catalysts, only ligands 2-(diphenylphospha-

2, 7, Downloaded from https://chemistry-europe.onlinelibrary.wiley.com/doi/10.1002/chem.202104102 by Texas Tech University Libraries, Wiley Online Library on [25/10/2022]. See the Terms and Conditions (https://onlinelibrary.wiley.com/terms

-and-conditions) on Wiley Online Library for rules of use; OA articles are governed by the applicable Creative Commons License

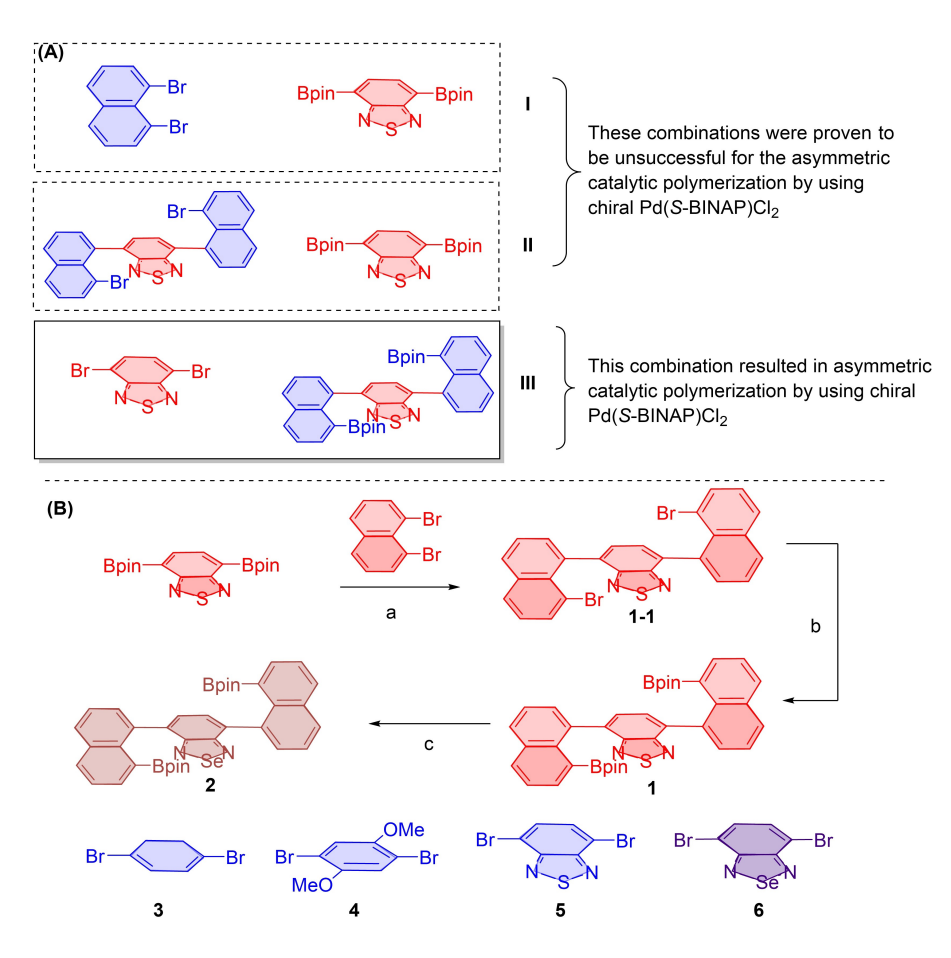


Figure 2. A) Retrosynthetic analysis. B) Monomer synthesis. Conditions: a)  $Pd(PPh_3)_4$ ,  $THF/H_2O$ ,  $K_2CO_3$ , 85 °C, 6 h, 79%; b)  $Pd(dppf)Cl_2$ , bis(pinacolato)diboron, dioxane, 108 °C, 12 h, 65%; c)  $NaBH_4$ ,  $CoCl_2 \cdot 6H_2O$ , THF/EtOH, RT, 4 h;  $SeO_2$ ,  $EtOH/H_2O$ , THF/EtOH, RT, 4 h;  $SeO_3$ ,  $SeCO_3$ , 85 °C, 6 h, 79%; b)  $Pd(dppf)Cl_2$ , bis(pinacolato)diboron, dioxane, 108 °C, 12 h, 65%; c)  $NaBH_4$ ,  $NaBH_4$ ,

neyl)-N,N-bis((R)-1-phenylethyl)benzamide and (S)-BINAP as well as the Pd(S-BINAP)Cl $_2$  complex showed catalytic activities; unexpectedly, Pd(S-BINAP)Cl $_2$  provided the best result with a chemical yield of 52% and optical rotation of  $[\alpha]_0^{20} = +80.8$ .

Six combinations of co-monomer pairs were examined showing a good substrate scope (Scheme 1). While S- and Se-based bridges were electron-deficient frames between bridge piers (naphthyl columns), neighboring layers could be coordinated to electron-enriched moieties with two MeO— groups attached. These differentiated-layer arrangements would be anticipated to meet different material demands in application studies, such as polarized organic electronics, optoelectronics,

photovoltaics, etc. As shown in Table 1, 1A, 2A, and 2C were synthesized in yields of 51%, 77%, and 12%, respectively. For these three products, gel permeation chromatography (GPC) analysis showed up to Mw of 61960 and Mn of 41500. 1B, 1C, and 2B were obtained in modest yields of 52, 62, and 36% in turn. However, they could only be analyzed by MALDI-TOF due to the poor solubility for GPC. Specifically, the highest mass (m/z) could be found at 4315, 3642, and 2146, indicating 17, 14, and 7 folding layers, accordingly, existed in these foldamers (Table 1).

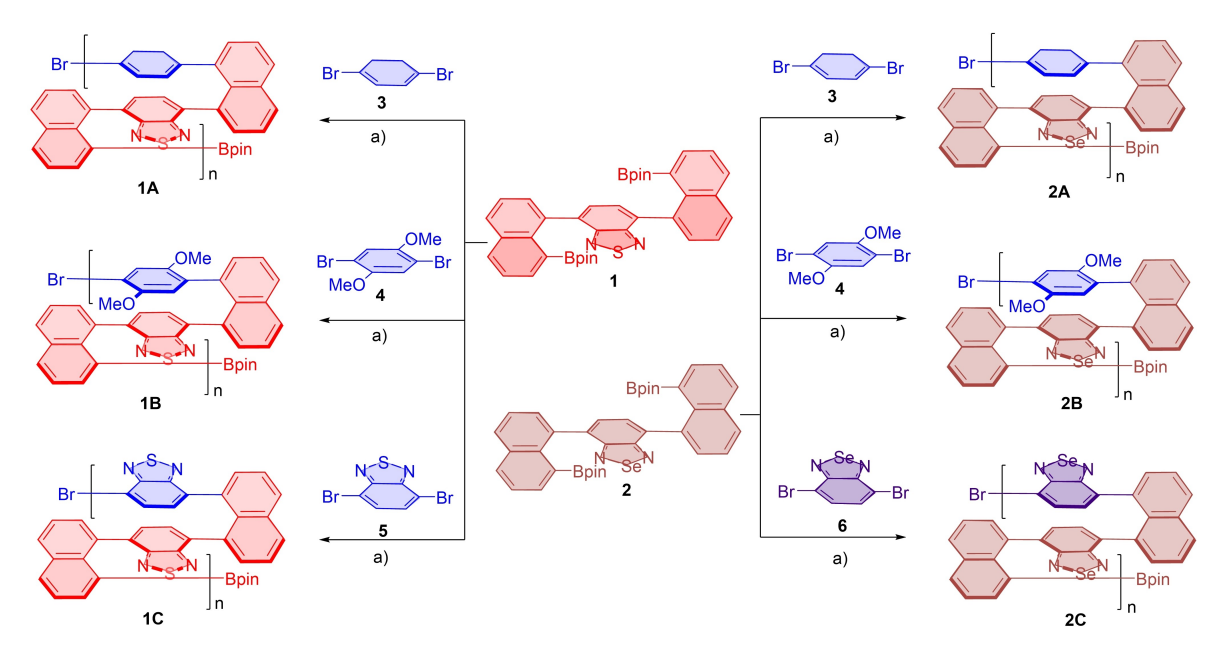
Our attempt to isolate pure oligomers to conduct X-ray structural analysis was unsuccessful due to the fact that there

Table 1. Results of synthetic chiral polymers.							
Poly-Prod.	Yield [%] <sup>[a]</sup>	$M_{\rm w}^{\rm [b]}$	$M_n^{[b]}$	PDI <sup>[c]</sup>	MALDI-TOF m/z <sup>[d]</sup>	Layers <sup>[d]</sup>	$[\alpha]_{\mathrm{D}}^{\mathrm{20[e]}}$
1A	51	54323	32378	1.678	_	-	+13.3 (c=0.06)
1B	52	-	-	-	4315	17	+80.8 (c=0.73)
1C	62	-	-	-	3642	14	-213.8 (c=0.14)
2A	77	57774	39835	1.450	_	-	+9.5 (c=0.20)
2B	36	-	-	-	2146	7	+2.7 (c=0.30)
2C	12	61960	41500	1.493	-	-	+ 1.6(c = 0.43)

[a] Isolated yield based on substrate 1 or 2. [b] Determined by GPC with a polystyrene standard. [c] PDI =  $M_w/M_n$ . [d] Calculated based MALDI-TOF data. [e] In CHCI3; c = g/100 mL.

2, 7, Dwnloaded from https://chemistry-erope onlinelibrary.viley.com/doi/10.1002/chem.202104102 by Texas Tech University Libraries, Wiley Online Library on [25/10/2022]. See the Terms and Conditions (https://onlinelibrary.wiley.com/ems

and-conditions) on Wiley Online Library for rules of use; OA articles are governed by the applicable Creative Commons License



Scheme 1. Catalytic coupling assembly of multilayer folding 3D chiral polymers 1A–2C. All reactions were carried out with substrates 1–6 (0.2 mmol), Pd(S-BINAP)Cl<sub>2</sub> (5 mol%) and and K<sub>2</sub>CO<sub>3</sub> (0.8 mmol) in THF/H<sub>2</sub>O (9.5:1.5 mL) for 6 days under Ar.

were too many species co-existing in the reaction mixtures, which made it extremely difficult to purify. However, the absolute stereochemistry of major enantiomers could be assigned by comparison with a similar stereoselective control by the same catalyst of Pd(S-BINAP)Cl<sub>2</sub>. This catalyst resulted in "S" folding of multilayer 3D enantiomers in our previous work, and was anticipated to give the same asymmetric induction in this catalytic process as shown in Figure 3B. [15e] It is noteworthy that this asymmetric induction resulted in a pseudo or prochiral center on phosphorus atom which is attributed to the orientation/rotation (or, orientational/rotational) chirality controlled by special scaffolds of naphthalenyl and benzo[c][1,2,5]-thiadizole rings

The diastereochemistry of products 1C and 2C were revealed as *anti-anti* or head-tail arrangements, that is, seleno/thiophene bridges are alternatively oriented (1C-t, 2C-d; Figure 3B). Notably, no other diastereoisomers were formed during racemic couplings as indicated by the three-layer diastereoselective control of dimers and trimers. Likewise, the diastereochemistry of polymeric products 1B and 2B could be assigned by X-ray diffractional analysis of mono-coupling intermediate 1B-d (Figure 3B).

The UV-Vis absorption spectra (Figure 4A) of six foldamers in chloroform exhibited two main maxima below 450 nm. For 1A–1C, the first absorption at 305 nm was much stronger than the second at 389 nm. However, both peaks on the bands of 2A–2C had slight longwave shifts, displayed an intense absorption at 318 nm and a significantly weaker absorption at 424 nm.

Photoluminescence (PL) studies were also performed for 1A–2C in THF with the same concentration (Figure 4B). The overall shapes of the six products are quite consistent. If the thiadiazole chromophore was replaced with the selenadiazole

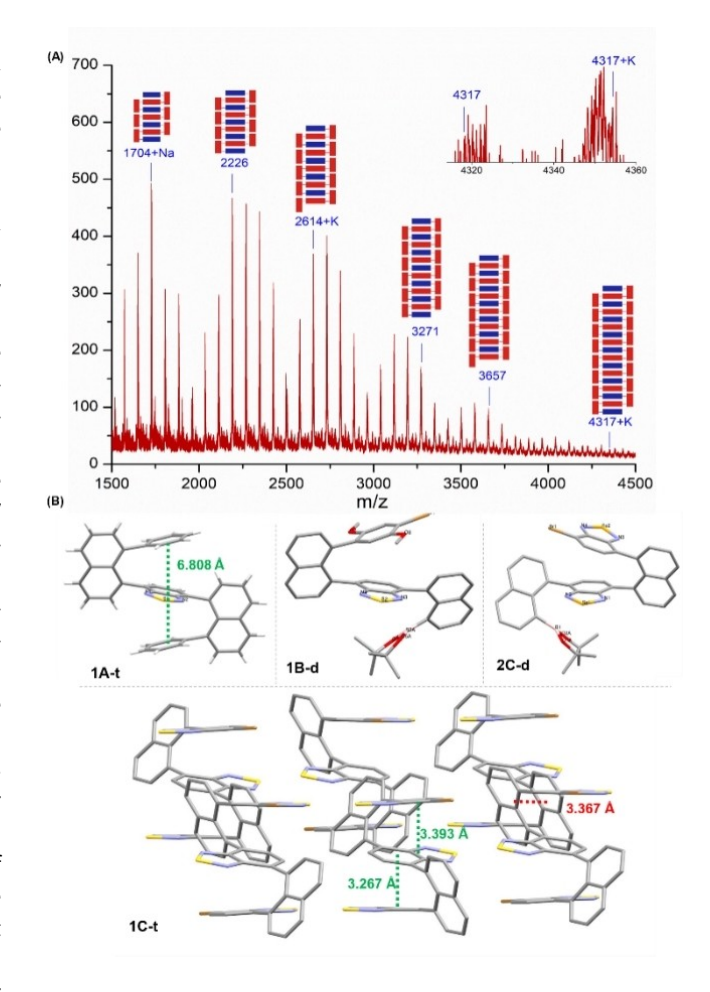


**Figure 3.** A) MALDI-TOF of chiral oligomers **1B**. B) Stereochemistry assignment by X-ray structural analysis.

2, 7, Downloaded from https://chemistry-europe.onlinelibrary.wiley.com/doi/10.1002/chem.202104102 by Texas Tech University Libraries, Wiley Online Library on [25/10/2022]. See the Terms and Conditions (https://onlinelibrary.wiley.com/ems-s-

and-conditions) on Wiley Online Library for rules of use; OA articles are governed by the applicable Creative Commons License

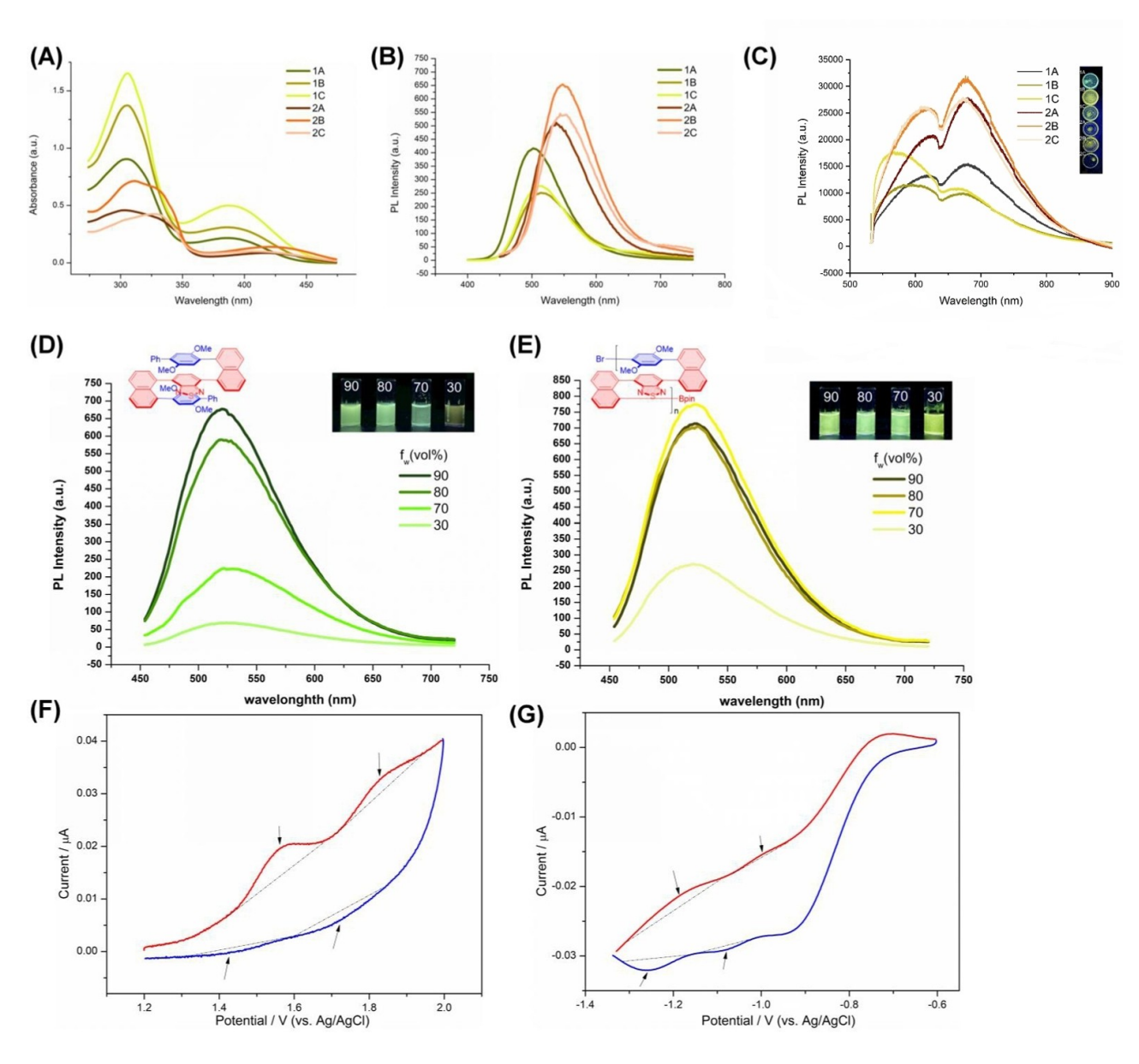


Figure 4. A) UV/Vis absorption spectra of 1A-2C in CHCl<sub>3</sub>;  $c=50 \, \mu g \, mL^{-1}$ . B) PL spectra of 1A-2C in THF;  $c=50 \, \mu g \, mL^{-1}$ ,  $\lambda_{ex}$  (1A, 1B, 1C) = 385 nm,  $\lambda_{ex}$  (2A, 2C) = 420 nm,  $\lambda_{ex}$  (2B) = 425 nm. C) PL spectra of solid samples 1A-2C;  $\lambda_{ex}=532$  nm; inset: top view of solid samples 1A-2C in scintillation vials under longwave UV (365 nm) irradiation. PL spectra of D) 1B-t and E) 1B in THF/water with different water fractions ( $f_w$ );  $c_{monomer}=0.1 \, mM$ ,  $c_{18}=50 \, \mu g \, mL^{-1}$ ;  $\lambda_{ex}$  (1B-t) = 380 nm,  $\lambda_{ex}$  (1B) = 385 nm; insets: fluorescence photographs of 1B-t and 1B in THF/water. Electrochemical performance of F) 2B and G) 2C in CH<sub>2</sub>Cl<sub>2</sub> containing 0.1 M Bu<sub>4</sub>NPF<sub>6</sub> as an electrolyte at 298 K; the scan rate is 100 mV s<sup>-1</sup>.

counterpart, a conversion of emission at 510 nm (1A–1C) into more prominent, red-shifted peaks at 540 nm (2A–2C) was observed.

Solid-state emission was evaluated in amorphous forms as well (Figure 4C). The PL spectra of six samples in the aggregated state showed pronounced red-shifted emission bands from those in the THF solutions. In particular, 1A, 2A, 2B and 2C showed distinct emissions at around 620 nm, followed by the main peaks at 680 nm. At the same time, both electron-donating and withdrawing substitutions on the thiadiazoles directed blue-shifts for 1B and 1C. The band maxima switched

from the second broad peaks to the first at 589 and 567 nm, respectively.

The comparison of AIE activities for enantioenriched oligomer 1B and the trimer 1B-t with the same skeleton was studied by fluorescence spectroscopy. In Figure 4D, the emission maxima of 1B-t were gradually increasing as the water fractions ( $f_w$ ) changed from 30 to 90%. In contrast, the emission intensity of polymer 1B was enhanced by leaps and bounds when the  $f_w$  increased to 70% (Figure 4E). This big jump could attribute to the suppression of molecular motion by intermolecular packing of the polymer matrix, indicating that this chiral multilayer framework undergoes AIE. However, as the  $f_w$ 

Chemistry Europe

European Chemical Societies Publishing

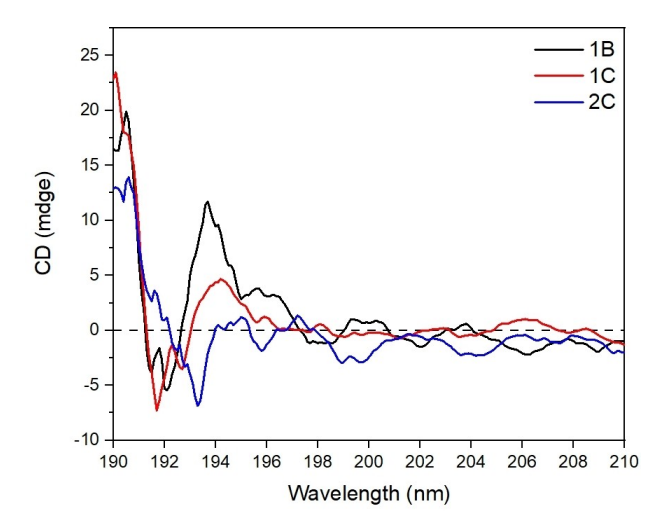


**Figure 5.** CD spectra of **1B**, **1C**, and **2C** in methanol;  $c = 0.2 \text{ mg mL}^{-1}$  (for CD spectra of the rest, see the Supporting Information).

continued to rise to 80% and 90%, the luminescence intensities were faintly weakened. A reasonable explanation was that in a dilute environment, the motions between polymeric molecules would be decreasing as the poor solvent (water) became more, although intramolecularly layered framework would be affected by the intermolecular packing process. As soon as the critical saturation value of  $f_{\rm w}\!=\!70\%$  was reached, the intramolecular  $\pi^-$  stacking would become more regular and dominant by suppressing the entire framework while keeping adding water to the mixture. This compacted packing model contributed to more effective through-space  $\pi^-\pi$  interactions, thus offsets

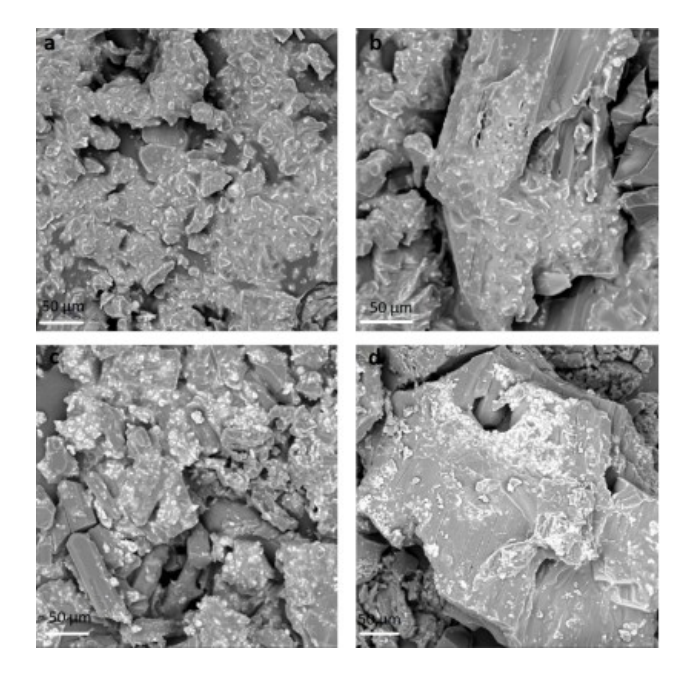


Figure 6. SEM images of chiral folding polymers 2B (top) and 2C (bottom).

partial AIE activities. This result was consistent with our previous study on racemic polymers.<sup>[15a]</sup>

Cyclic voltammetry measurements of selected samples were performed to investigate the redox property. Figure 4F and G showed the electrochemical performance of selenadiazole based foldamers **2B** and **2C**. As can be seen, both curves exhibited two reversible redox peaks. The simultaneous occurrence of oxidation and reduction peaks indicated that these multiple  $\pi$ -assemblies possessed electrons donation and acceptance capabilities. For **2B**, specifically, the oxidation peaks at 1.57 and 1.82 V; while two reduction peaks loomed at 1.70 and 1.44 V. Compared to the oxidation peaks, the reduction peaks of **2B** were less noticeable though. **2C** had two oxidation peaks occurred at -1.18 and -0.99 V; correspondingly, two reduction peaks were located at -1.08 and -1.26 V. One thing should be aware that the peaks at -0.93 V were from supporting electrolyte (Figure S8).

The optical activities of selected chiral folding polymers 1B, 1C and 2C were further studied by CD spectroscopies. As exhibited in Figure 5, polymer 1B showed negative Cotton effects in the ranges of 204–206, 200–202, 194–198, and <192 nm, while it showed positive Cotton effects in the ranges of 202–204, 198–200, and 192–194 nm. Similar phenomena attributed to the aromatic rings from polymer backbone can be observed on polymer 1C either. However, polymer 2C displayed negative Cotton effects centered at about 193 nm and gradually turned to positive Cotton effects. CD spectra of chiral folding polymer 1A, 2A, and 2B is shown in the Supporting Information.

Morphological studies of chiral folding polymers were performed by scanning electron microscopy (SEM) as described in Figure 6. Solid polymer samples were coated with a thin gold layer to increase the conductivity and decrease the signal-to-noise ratio. Selected chiral polymer **2B** (Figure 6a and b) and **2C** (Figure 6c and d) exhibited cauliflower-like structures on their surface, bearing a nonuniform distribution of homogeneous balls with lengths roughly 2 to 10  $\mu$ m in diameter. Compared with polymer **2C**, **2B** had a smoother surface with fewer particles.

## Conclusion

In summary, we have successfully synthesized six chiral triple-columned/multilayered 3D folding polymers, stacking up to at least seven layers by different aromatic bridges. The absolute stereochemistry was assigned by X-ray analysis of individual micromolecules with a similar asymmetric induction by the same catalyst. CD spectra and scanning electron micrographs of these new chiral polymers have been obtained; they showed positive Cotton effects and exhibited cauliflower-like structures on their surface, bearing a nonuniform distribution of homogeneous balls. The insights of UV/Vis, fluorescence, electrochemical performance and especially the AIE properties showed that this work could provide new possibilities for chiral materials in the future.

#### Chemistry Europe European Chemical Societies Publishing

## **Experimental Section**

For experimental details, see the Supporting Information.

Crystal-structure analysis: Deposition Numbers 2097094 (for 1A-t), 2097096 (for 2B-d) and 2130458 (for 2C-d) contain the supplementary crystallographic data for this paper. These data are provided free of charge by the joint Cambridge Crystallographic Data Centre and Fachinformationszentrum Karlsruhe Access Structures service.

# **Acknowledgements**

This work was supported by the Robert A. Welch Foundation (D-1361-20210327, USA), and the National Natural Science Foundation of China (22071102 and 91956110). We thank Dr. Yangxue Liu and Liulei Ma for their assistance with syntheses; Prof. K. Hutchins and Q.-X. Zheng for their assistance with the GPC analysis; Prof. C. Korzeniewski and J. Xu for their assistance with the cyclic voltammetry measurements; Profs. Y. Mechref and S.-Y. Wang as well as Drs. X. Gong and M. Zabet for their assistance with the MALDI-TOF analysis and helpful discussions.

### **Conflict of Interest**

The authors declare no conflict of interest.

# **Data Availability Statement**

The data that support the findings of this study are available from the corresponding author upon reasonable request.

**Keywords:** aggregation-induced emission (AIE) · asymmetric catalytic polymerization · chirality · multilayer chiral polymers · Suzuki-Miyaura coupling

- [1] a) H. E. Moser, P. B. Dervan, Science 1987, 238, 645-650; b) K. W. Knouse, N. Justine, M. A. Schmidt, B. Zheng, J. C. Vantourout, C. Kingston, S. E. Mercer, I. M. Mcdonald, R. E. Olson, Y. Zhu, Science 2018, 361, 1234-1238; c) H. Gong, J. Li, A. Xu, Y. Tang, W. Ji, R. Gao, S. Wang, L. Yu, C. Tian, J. Li, H. Yen, S. M. Lam, G. Shui, X. Yang, Y. Sun, X. Li, M. Jia, C. Yang, B. Jiang, Z. Lou, C. V. Robinson, L. Wong, L. W. Guddat, F. Sun, Q. Wang, Z. Rao, Science 2018, 362, 6418.
- [2] a) E. J. Corey, B. Czakó, L. Kürti, Molecules and Medicine, John Wiley & Sons, 2012; b) K. Nicolau, S. Snyder, Classics in Total Synthesis II, Wiley-VCH, Weinheim, 2003; c) H. Yamamoto, E. M. Carreira, Comprehensive Chirality: Online, Elsevier Science, 2012; d) E. N. Jacobsen, A. Pfaltz, H. Yamamoto, Comprehensive Asymmetric Catalysis, Supplement 1, Vol. 1, Springer, 2003; e) I. Ojima, Catalytic Asymmetric Synthesis, Wiley, 2010.
- [3] a) Y. Wu, M. Frasconi, D. M. Gardner, P. R. McGonigal, S. T. Schneebeli, M. R. Wasielewski, J. F. Stoddart, Angew. Chem. Int. Ed. 2014, 53, 9476-9481; Angew. Chem. 2014, 126, 9630-9635; b) S. K. Keshri, T. Ishizuka, T. Kojima, Y. Matsushita, M. Takeuchi, J. Am. Chem. Soc. 2021, 143, 3238-3244; c) S. K. Keshri, W. Nakanishi, A. Takai, T. Ishizuka, T. Kojima, M. Takeuchi, Chem. Eur. J. 2020, 26, 13288-13294.
- [4] a) T. Nakano, Polym. J. 2010, 42, 103-123; b) Y. Morisaki, J. A. Fernandes, Y. Chujo, Polym. J. 2010, 42, 928-934; c) F. Chen, J. Hu, X. Wang, S. Shao, L. Wang, X. Jing, F. Wang, Sci. China Chem. 2020, 63, 1112–1120.
- [5] P. Saura, V. R. Kaila, J. Am. Chem. Soc. 2019, 141, 5710-5719.
- [6] M. Chen, Y. Jun Bea, C. M. Mauck, A. Mandal, R. M. Young, M. R. Wasielewski, J. Am. Chem. Soc. 2018, 140, 9184-9192.

- [7] a) C.-F. Chen, Y. Shen, Helicene Chemistry: From Synthesis to Applications, Springer, 2017; b) I. G. Stará, I. Starý, Acc. Chem. Res. 2020, 53, 144-158; c) Y. Shen, C.-F. Chen, Chem. Rev. 2012, 112, 1463-1535.
- [8] a) T. Kawashima, Y. Matsumoto, T. Sato, Y. M. A. Yamada, C. Kono, A. Tsurusaki, K. Kamikawa, Chem. Eur. J. 2020, 26, 13170-13176; b) K. Fujise, E. Tsurumaki, K. Wakamatsu, S. Toyota, Chem. Eur. J. 2021, 27, 4548-4552.
- [9] a) Y. Morisaki, Y. Chujo, Tetrahedron Lett. 2005, 46, 2533-2537; b) Y. Morisaki, T. Murakami, T. Sawamura, Y. Chujo, Macromolecules 2009, 42, 3656-3660.
- [10] a) S. P. Jagtap, D. M. Collard, J. Am. Chem. Soc. 2010, 132, 12208-12209; b) S. P. Jagtap, D. M. Collard, Polym. Chem. 2012, 3, 463-471; c) Y. Morisaki, J. A. Fernandes, Y. Chujo, Polym. J. 2010, 42, 928-934.
- [11] a) K. Oh, K.-S. Jeong, J. S. Moore, Nature 2001, 414, 889-893; b) D. J. Hill, M. J. Mio, R. B. Prince, T. S. Hughes, J. S. Moore, Chem. Rev. 2001, 101, 3893-4012.
- [12] a) S. H. Gellman, Acc. Chem. Res. 1998, 31, 173-180; b) J. M. Tour, Acc. Chem. Res. 2000, 33, 791-804.
- [13] a) Y.-N. Lin, M. Elsabahy, S. Khan, F. Zhang, Y. Song, M. Dong, R. Li, J. Smolen, R. A. Letteri, L. Su, ACS Mater. Lett. 2020, 2, 595-601; b) X. Xie, P. W. Phuan, M. C. Kozlowski, Angew. Chem. Int. Ed. 2003, 42, 2168-2170; Angew. Chem. 2003, 115, 2218-2220.
- [14] a) M. Nishiura, F. Guo, Z. Hou, Acc. Chem. Res. 2015, 48, 2209-2220; b) Y. Yang, M. Nishiura, H. Wang, Z. Hou, Coord. Chem. Rev. 2018, 376, 506-
- [15] a) G. Wu, Y. Liu, Z. Yang, L. Ma, Y. Tang, X. Zhao, H. Rouh, Q. Zheng, P. Zhou, J-Y. Wang, F. Siddique, S. Zhang, S. Jin, D. Unruh, A. J. A. Aquino, H. Lischka, K. M. Hutchins, G. Li, Research 2021, 2021, 3565791; b) G. Wu, Y. Liu, Z. Yang, T. Jiang, N. Katakam, H. Rouh, L. Ma, Y. Tang, S. Ahmed, A. U. Rahman, G. Li, Natl. Sci. Rev. 2020, 7, 588-599; c) Y. Liu, G. Wu, Z. Yang, H. Rouh, N. Katakam, S. Ahmed, D. Unruh, Z. Cui, H. Lischka, G. Li, Sci. China Chem. 2020, 63, 692-698; d) J.-L. Zhang, L. Kürti, Natl. Sci. Rev. 2021, 8, nwaa205; e) G. Wu, Y. Liu, H. Rouh, L. Ma, Y. Tang, S. Zhang, P. Zhou, J. Wang, S. Jin, D. Unruh, K. Surowiec, Y. Ma, G. Li, Chem. Eur. J. **2021**, 27, 8013-8020.
- [16] a) G. An, C. Seifert, G. Li, Org. Biomol. Chem. 2015, 13, 1600–1617; b) J.-B. Xie, J. Luo, T. R. Winn, D. B. Cordes, G. Li, J. Org. Chem. 2014, 10, 746-751; c) P. Kaur, W. Wever, S. Pindi, R. Milles, P. Gu, M. Shi, G. Li, Green Chem. 2011, 13, 1288-1292.
- [17] a) C. W. Seifert, A. Paniagua, G. A. White, L. Cai, G. Li, Eur. J. Org. Chem. 2016, 1714–1719; b) P. Kaur, S. Pindi, W. Wever, T. Rajale, G. Li, J. Org. Chem. 2010, 75, 5144-5150; c) "New Synthetic Methodology for Chiral Amines and Peptides via GAP Technology", C. Seifert, Ph.D. Thesis, Texas Tech University (USA), 2017.
- [18] a) A. S. Guram, S. L. Buchwald, J. Am. Chem. Soc. 1994, 116, 7901-7902; b) F. Paul, J. Patt, F. J. Hartwig, J. Am. Chem. Soc. 1994, 116, 5969-5970.
- [19] a) N. Miyaura, A. Suzuki, Chem. Rev. 1995, 95, 2457-2483; b) A. Kumar, S. Bawa, K. Ganorkar, S. K. Ghosh, A. Bandyopadhyay, Inorg. Chem. 2020, 59, 1746-1757.
- [20] a) J. Li, P. Shen, Z. Zhao, B. Z. Tang, CCS Chemistry 2019, 1, 181-196; b) N. G. X. Zheng, Z. Zhao, H. Zhang, J. Wang, X. He, Y. Chen, X. Shi, C. Ma, R. T. K. Kwok, J. W. Y. Lam, H. H. Y. Sung, I. D. Williams, K. S. Wong, P. Wang, B. Z. Tang, J. Am. Chem. Soc. 2019, 141, 15111-15120; c) L. Xu, Z. Wang, R. Wang, L. Wang, X. He, H. Jiang, H. Tang, D. Cao, B. Z. A. Tang, Angew. Chem. Int. Ed. 2020, 59, 9908-9913; Angew. Chem. 2020, 132, 9994-9999.
- [21] E. J. Corey, X.-M. Cheng, The Logic of Chemical Synthesis, Wiley-Interscience, New York, 1995.
- [22] B. A. DaSilveira Neto, A. S. Lopes, M. Wüst, V. E. U. Costa, G. Ebeling, J. Dupont, Tetrahedron Lett. 2005, 46, 6843-6846.
- [23] I. Idris, T. Tannoux, F. Derridj, V. Dorcet, J. Boixel, V. Guerchais, J. F. Soule, H. Doucet, J. Mater. Chem. C. 2018, 6, 1731-1737.
- [24] M. Echeverri, C. Rui, S. Gámez-Valenzuela, M. Alonso-Navarro, E. Gutierrez-Puebla, J. L. Serrano, M. Carmen Ruiz Delgado, B. Gómez-Lor, ACS Appl. Mater. Interfaces 2020, 12, 10929-10937.
- [25] a) S. Vyskocil, L. Meca, I. Tislerová, I. Císarová, M. Polásek, S. R. Harutyunyan, Y. N. Belokon, R. M. Stead, L. Farrugia, S. C. Lockhart, W. L. Mitchell, P. Kocovský, Chem. Eur. J. 2002, 8, 4633-4648; b) R. Jurok, R. Cibulka, H. Dvořáková, F. Hampl, J. Hodačová, Eur. J. Org. Chem. 2010, 2010, 5217-5224.

Manuscript received: November 15, 2021 Accepted manuscript online: December 28, 2021 Version of record online: January 19, 2022

and-conditions) on Wiley Online Library for rules of use; OA articles are governed by the applicable Creative Commons License